CHEMISTRY OF MATERIALS

ARTICLE

pubs.acs.org/cm

SERS-Active Nanoparticles for Sensitive and Selective Detection of Cadmium Ion (Cd^{2+})

Jun Yin,[†] Tao Wu,[‡] Jibin Song,[†] Qian Zhang,[†] Shiyong Liu,[*,‡] Rong Xu,[†] and Hongwei Duan[*,†]

[†]School of Chemical and Biomedical Engineering, Nanyang Technological University, 70 Nanyang Drive, Singapore 637457

[‡]CAS Key Laboratory of Soft Matter Chemistry, Department of Polymer Science and Engineering, Hefei National Laboratory for Physical Sciences at the Microscale, University of Science and Technology of China, Hefei, Anhui 230026, China

ABSTRACT: We report a new class of turn-on surface enhanced Raman scattering (SERS) sensors for the sensitive and selective detection of cadmium ion (Cd^{2+}) by taking advantage of the interparticle plasmonic coupling generated in the process of Cd^{2+}-selective nanoparticle self-aggregation. The SERS-active nanoparticles consist of 41-nm gold nanoparticles, encoded with a Raman-active dye through a disulfide anchoring group, and a layer of Cd^{2+}-chelating polymer brush coating grafted on the nanoparticle via surface-initiated atom transfer radical polymerization. These SERS nanoparticles are optimized to remain spectrally silent when staying as single particles. Addition of Cd^{2+} leads to interparticle self-aggregation and immediately turns on the SERS fingerprint signal with up to 90-fold of signal enhancement. The selectivity of the SERS nanoparticle for Cd^{2+} was also examined, showing that various common metal ions cannot induce interparticle self-aggregation and the turn-on of SERS signal. In contrast to nanoparticle-based colorimetric assays, the SERS probe is also capable of detecting Cd^{2+} in heavily colored samples.

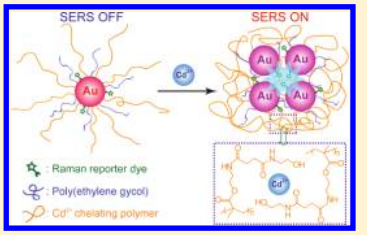

KEYWORDS: SERS, metal nanoparticles, nanosensors, cadmium ion, SI-ATRP

1. INTRODUCTION

Metal ion sensors are of considerable current interest for a broad range of biological and environmental applications.[1−3] It has been increasingly recognized that certain metal ions such as Zn^{2+} are essential nutrients to maintain regular cell functions.[2,3] On the other hand, the chronic and acute exposure to toxic heavy metal ions such as Cd^{2+}, Pb^{2+}, and Hg^{2+} can exert direct impact on human health and are linked to major human diseases such as cancer and cardiovascular disease.[4,5] Highly sensitive and selective methods for the detection of metal ions not only can provide insight into the physiological activity of metal ions but also are in great demand for waste management and food safety screening. Technologies such as atomic absorption spectrophotometry, fluorescence spectroscopy, and electrochemical analysis have been commonly used to detect metal ions present in biological or environmental specimens.[6−12] However, selectivity, long-term stability, compatibility with aqueous environments, and easiness for on-site sampling remain significant challenges for many of these techniques.

Recent advances in nanotechnology have led to the development of new detection mechanisms for the design of metal ion sensors.[13−22] For example, localized surface plasmon resonance (LSPR) of gold or silver nanoparticles exhibits sizable red-shifts upon forming nanoparticle aggregates because of interparticle plasmonic coupling.[23−25] The spectral shift coupled with the high extinction coefficient of metal nanoparticles allows for the development of colorimetric sensors based on metal nanoparticles with surface coatings responsive to specific metal ions.[13−22] These colorimetric nanosensors can address intrinsic limitations of small molecular dye-based fluorescent sensors such as the fluorescence quenching by metal ions and poor photostability. However, their practical uses in media exhibiting strong absorption of visible light are still problematic.

The other detection mechanism that benefits from the target-specific self-aggregation of metal nanoparticles is surface enhanced Raman scattering (SERS).[26−28] SERS has emerged as a powerful technique with extraordinary sensitivity for applications in a number of chemical and biological systems.[26−33] Accumulating evidence have demonstrated that the SERS signal of Raman dyes tagged on the nanoparticles can be significantly enhanced by the interparticle plasmonic coupling induced by the aggregation of metal nanoparticles .[34,35] The enhancement resulting from the aggregation of SERS-active nanoparticles carrying single-strand DNA probes has been employed to track DNA hybridization, allowing the detection of target DNA with single base accuracy.[36,37] Recently, Nie et al. reported the fabrication of stimuli-responsive SERS nanoparticles coated with block copolymer brushes, in which the pH-sensitive conformational change of poly(methacrylic acid) block can reversibly modulate the intensity of Raman signals in a off-on switchable manner.[38]

Here, we report a new class of sensitive and selective turn-on SERS sensors for Cd^{2+} by taking advantage of the plasmonic coupling generated in the process of Cd^{2+}-selective nanoparticle self-aggregation. Our design of SERS nanoparticles consists of 41-nm gold nanoparticles, encoded with a Raman-active dye through a disulfide anchoring group, and a layer of Cd^{2+}-chelating

Received: June 23, 2011
Revised: September 23, 2011
Published: October 13, 2011

polymer brush coating grafted on the nanoparticle via surface-initiated atom transfer radical polymerization (SI-ATRP). Previous reports have suggested that the extent of SERS signal amplification by single metal nanoparticles is closely correlated to the size of the nanoparticle, the average number of SERS dyes on the particle, and the laser excitation wavelength of choice.[37] In this study, the SERS-active nanoparticles are optimized to remain spectrally silent when staying as single particles. SI-ATRP offers the flexibility of growing a host of densely grafted polymer brushes of functional monomers on nanoparticles with defined sizes and geometry.[39−41] The polymer coating in this design plays dual roles of stabilizing the nanoparticles against nonspecific aggregation and recognizing Cd^{2+} through specific metal−ligand interaction, and the latter leads to fast interparticle aggregation. Our results have shown that SERS fingerprint signal can be sensitively and selectively turned on by Cd^{2+} among a group of competing metal ions including Zn^{2+}, which has been the main source of interference for Cd^{2+} detection due to their similar chemical properties and electronic structures.[7−9] The current work represents a proof-of-concept example of utilizing Raman-active dye encoded nanoparticles for the detection of metal ions.

2. EXPERIMENTAL SECTION

Methoxypoly(ethylene glycol)thiol (PEG-SH) with a molecular weight of 2000 Da was purchased from Laysan Bio, Inc. Chloroauric acid and *n*-butyllithium (2.88 M solution in hexane) were obtained from Alfa Aesar. Succinic anhydride, 2-aminoethanol, 2-aminoethyl methacrylate hydrochloride, *N*-hydroxysuccinimide (NHS), *N*,*N*′-dicyclohexylcarbodiimide (DCC), 4-bromophenol, 2-bromoethanol, methyl 2-bromopropinate, and 4,4′-bis-(*N*,*N*-diethyl amino)benzophenone were purchased from Sigma-Aldrich and used as received. 2,2′-Dithiobis [1-(2-bromo-2-methyl-propionyloxy)]ethane (DTBE) was synthesized according to our previous report.[42] Tris(2-(dimethylamino)ethyl)amine (Me_6TREN) was prepared according to literature procedures.[43] Water was deionized with a Milli-Q SP reagent water system (Millipore) to a specific resistivity of 18.0 MΩcm. All the other chemical reagents were obtained from commercial suppliers and used without further purification.

^{1}H NMR characterization was conducted at Bruker AV300, using $CDCl_3$ and D_2O as solvents. SERS measurements were implemented on a PeakSeeker Pro (Agiltron) Raman system using an excitation laser with 785 nm wavelength at 100 mW. Raman spectra were collected in the wavenumber range of 200−2000 cm^{-1} for an integration time of 10 s, calibrated with a silicon standard at 520 cm^{-1}. Peak heights for the SERS spectral band at 525 cm^{-1} were determined by taking the difference between the peak intensity maximum and an average baseline for each spectrum. The enhancement factor was calculated by using the signal from single particles as the background signal. UV−vis absorption spectra were recorded by using a Thermo Electron UV−vis spectrophotometer (NICOLET evolution 500). Transmission Electron Microscopy (TEM) observations were conducted on a Jeol JEM 2010 electron microscope at an acceleration voltage of 300 kV. Gel permeation chromatography (GPC) was measured on a Shimadzu HPLC system using $CHCl_3$ as the eluent, and the molecular weight is calibrated with polystyrene standards.

Synthesis of Gold Nanoparticles. Uniform 13-nm gold nanoparticles were prepared by citrate reduction of $HAuCl_4$ in aqueous solutions. Typically, a sodium citrate (102 mg) DI water solution (2 mL) was rapidly injected into a boiling aqueous $HAuCl_4$ (30 mg in 200 mL of DI water) solution under vigorous stirring. After boiling for 15 min, the solution was cooled to room temperature. Gold nanoparticles with an average diameter of 41 nm were synthesized using 13 nm nanoparticles as seeds. Briefly, a freshly prepared aqueous $HAuCl_4$ solution (20 mg in 100 mL of DI water) was heated to boiling, followed by the sequential injection of the as-prepared seed solution (8 mL, 13-nm Au nanoparticles) and sodium citrate solution (0.56 mL, 20 g/L) under vigorous stirring. The mixed solution was then heated for another 30 min before cooled down to room temperature.

Synthesis of 2-(4-Bromophenoxy)ethanol. A mixture of K_2CO_3 (30.0 g, 0.22 mol), 4-bromophenol (30.0 g, 0.17 mol), and 2-bromoethanol (31.0 g, 0.25 mol) in acetone (500 mL) was refluxed under N_2 for 48 h. Then, the mixture was filtered and evaporated to dryness. CH_2Cl_2 was added to dissolve the products and then washed with brine. The organic phase was dried over anhydrous $MgSO_4$. After the insoluble solids were removed by suction filtration, the CH_2Cl_2 solution was concentrated using a rotary evaporator. The crude product was further purified by silica gel column chromatography using ethyl acetate/petroleum ether (1:2, v/v) as the eluent. After removing all the solvents, the product was obtained as a white solid (22.14 g, yield: 60%). ^{1}H NMR ($CDCl_3$, δ, ppm, TMS): 7.39 and 6.81 (4H, *phenyl*), 4.05 (2H, $-OCH_2CH_2OH$), and 3.96 (2H, $-OCH_2CH_2OH$).

Synthesis of 2-(4-(Bis(4-(diethylamino)phenyl)(hydroxy)-methyl)phenoxy)ethanol (1). This compound was synthesized according to literature procedures with little modification.[44] In a typical run, 2-(4-bromophenoxy)ethanol (4.0 g, 18.4 mmol) was dissolved in 100 mL of anhydrous THF under nitrogen atmosphere. The solution was cooled to −70 °C in a bath of liquid nitrogen and acetone. *n*-Butyllithium (12.8 mL of a 2.88 M solution in hexane, 36.8 mmol) was added with a syringe dropwise under continuous stirring. The mixture was left at −70 °C for 15 min. Then, 4,4′-bis-(*N*,*N*-diethylamino)-benzophenone (6.0 g, 18.4 mmol) was added as a solid under stirring, and the mixture was allowed to warm to room temperature and left for 2 h. Saturated solution of $NaHCO_3$ (100 mL) was added to quench the reaction, and ethyl acetate (100 mL) was used to extract the crude product. The organic phase was washed with 100 mL of brine and dried over anhydrous $MgSO_4$. The insoluble solids were removed by suction filtration, and ethyl acetate was concentrated using a rotary evaporator. The crude product was further purified by silica gel column chromatography using petroleum ether/ethyl acetate (1:3, v/v) as the eluent. After removing all the solvents, the product, **1**, was obtained as a green solid (4.26 g, yield: 50%). ^{1}H NMR ($CDCl_3$, δ, ppm, TMS): 7.25−6.57 (12H, *phenyl*), 4.07 (2H, $-OCH_2CH_2OH$), 3.94 (2H, $-OCH_2CH_2OH$), 3.32 (8H, $-N(CH_2CH_3)_2$), 1.99 (1H, $-OCH_2CH_2OH$), and 1.14 (12H, $-N(CH_2CH_3)_2$).

Synthesis of 2-(4-(Bis(4-(diethylamino)phenyl)(hydroxy)-methyl)phenoxy)ethyl 5-(1,2-Dithiolan-3-yl)pentanoate (BGLA, 2). A 50 mL round-bottom flask was charged with lipoic acid (0.76 g, 3.7 mmol), DCC (0.76 g, 3.7 mmol), and anhydrous CH_2Cl_2 (15 mL). The reaction mixture was cooled to 0 °C in an ice−water bath, and a solution of **1** (1.50 g, 3.2 mmol), DMAP (0.05 g, 0.4 mmol), and anhydrous CH_2Cl_2 (15 mL) was added dropwise over a period of 1 h under magnetic stirring. After the addition was completed, the reaction mixture was stirred at 0 °C for 1 h and then allowed to warm to room temperature for 12 h. After removing the insoluble salts by suction filtration, the filtrate was concentrated and further purified by silica gel column chromatography using petroleum ether/ethyl acetate (1:6, v/v) as an eluent. After removing all the solvents, the product, **2**, was obtained as a green solid (1.25 g, yield: 60%). ^{1}H NMR ($CDCl_3$, δ, ppm, TMS): 7.25−6.57 (12H, *phenyl*), 4.41 (2H, $-OCH_2CH_2OCO-$), 4.15 (2H, $-OCH_2CH_2OCO-$), 3.32 (8H, $-N(CH_2CH_3)_2$), 2.58−1.52 (12H, *lipoic acid*), and 1.14 (12H, $-N(CH_2CH_3)_2$).

Synthesis of 4-(2-Hydroxyethylamino)-4-oxobutanoic acid (HEBA, 3).[45]. Succinic anhydride (4.0 g, 0.04 mol) and 2-aminoethanol (2.44 g, 0.04 mol) were dissolved in 10 mL of acetone, respectively. The reaction took place under ice−water bath, and both of the acetone solutions were added to a three-neck bottle which contained 20 mL of acetone. The solutions were added slowly in about 30 min, and

dx.doi.org/10.1021/cm201791r |*Chem. Mater.* 2011, 23, 4756–4764

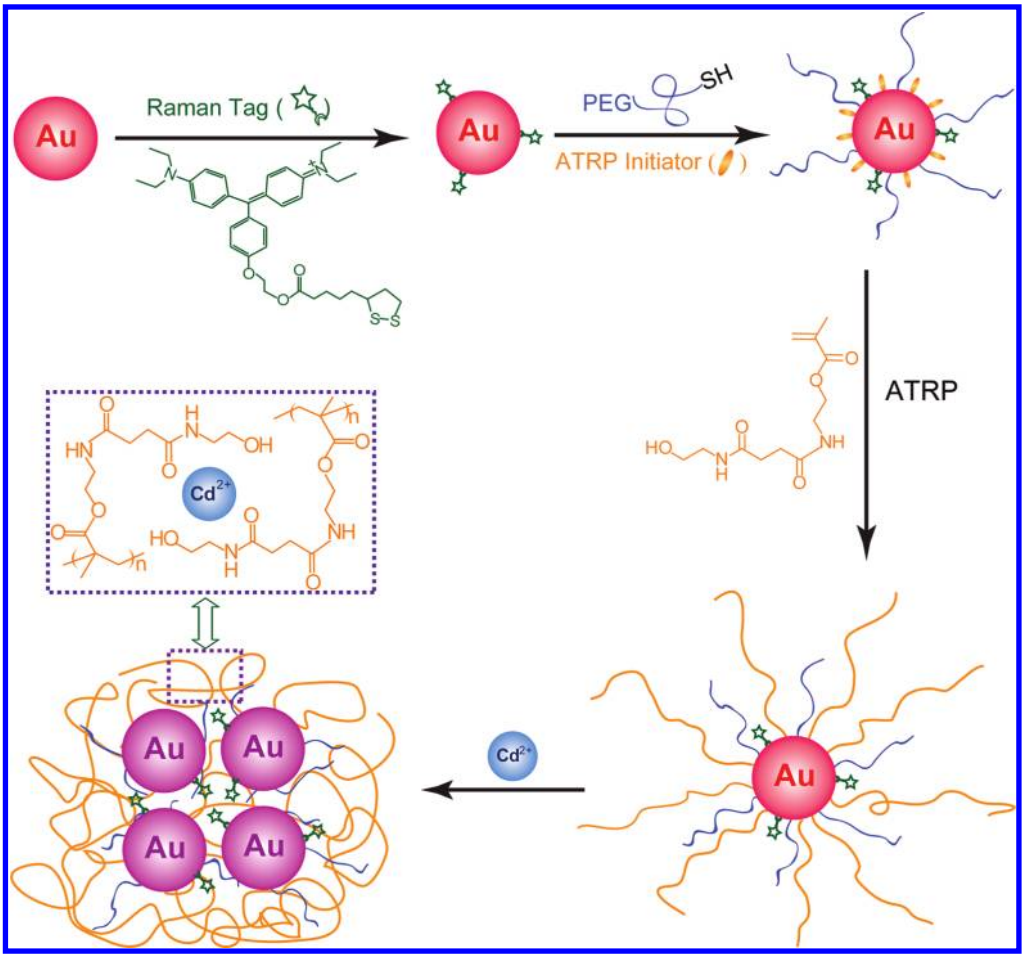

Figure 1. Schematic illustration of the procedure employed for the fabrication of SERS dye encoded gold nanoparticles *via* ligand exchange and surface-initiated ATRP and the working mechanism for selective Cd^{2+} recognition and binding.

then the reaction system was stirred for another 2 h. After all solvents were removed, the crude product, **3**, was obtained and used without further purification for later synthesis. ^{1}H NMR (D_2O, δ, ppm): 3.53 (2H, $HOCH_2CH_2NHCO-$), 3.23 (2H, $HOCH_2CH_2NHCO-$), and 2.44−2.50 (4H, $-NHCO(CH_2)_2COOH$).

Synthesis of 2-(4-(2-Hydroxyethylamino)-4-oxobutanamido)ethyl methacrylate (HEBAMA, 4). DCC (4.50 g, 0.022 mol) and **3** (3.22 g, 0.02 mol) were dissolved in 20 mL of ice-cold DMSO. After the solid was dissolved, NHS (2.53 g, 0.022 mol) was added in the solution. The reaction mixture was stirred continuously for 10 h at room temperature. Then, 2-aminoethyl methacrylate hydrochloride (3.31 g, 0.02 mol) and 2.5 mL of NEt_3 were added. After the mixture was stirred for another 5 h, 60 mL of ethyl acetate was added, the insoluble salts were removed by suction filtration, and the filtrate was washed with water (5 × 50 mL) to remove the excess salts and DMSO. The organic layers were dried over anhydrous Na_2SO_4, and ethyl acetate was concentrated using a rotary evaporator. The crude product was further purified by silica gel column chromatography using *n*-hexane/ethyl acetate (1:1, v/v) as an eluent. After removing all the solvents, the product, **4**, was obtained as a light yellow liquid (3.15 g, yield: 57.8%). ^{1}H NMR ($CDCl_3$, δ, ppm, TMS): 8.02 (2H, $-NHCOCH_2CH_2CONH-$), 6.13 and 5.60 (2H, $CH_2{=}C(CH_3)$-$COO-$), 4.23 (2H, $-COOCH_2CH_2NHCO-$), 3.55−3.48 (4H, HO-$(CH_2)_2NHCO-$), 3.20 (2H, $-COOCH_2CH_2NHCO-$), 2.52 (4H, $-NHCO(CH_2)_2CONH-$), and 2.04 (3H, $CH_2{=}C(CH_3)COO-$).

Preparation of SERS Dye Encoded Gold Nanoparticle-Based ATRP Initiator. Gold nanoparticle-based ATRP initiator was prepared by a series of ligand exchange reactions. In a typical procedure, a freshly prepared reporter solution of **4** (2 mL, 6.0 μM; BGLA final concentration not exceeding 0.24 μM) was added dropwise to a rapidly stirring 50 mL Au colloid (41-nm) over 5 min, and then stirring was continued for another 20 min, to make sure of the sufficient adsorption of reporter molecules onto Au surface. Subsequently, PEG-SH (MW = 2000 Da, 5 mg) and DTBE (6 mg) in DMF (2 mL) were added. After having been stirred for 48 h, the solution was centrifuged (5000 g for 10 min) to recover the nanoparticles (Au@BGLA/PEG/DTBE). The supernatant was discarded, and the nanoparticles were redispersed in DMF for further uses.

Preparation of Polymer Grafts Coated SERS-Active Gold Nanoparticles Using Surface-Initiated ATRP. Typically, to a Schlenk tube equipped with a magnetic stirring bar, **4** (0.4 g, 1.1 mmol), Au@BGLA/PEG/DTBE (1 mL, 3.0 nM), and a suitable amount of free initiator, methyl 2-bromopropinate, were dissolved in DMF (1 mL). After the mixture was degassed for 30 min by N_2, CuBr (4.0 mg) and Me_6TREN (30.0 μL) were added, and the reaction mixture was allowed to degas for another 5 min and then kept in a 50 °C oil bath for 16 h. After purification by centrifugation (6000 g for 10 min), the SERS-active Au@BGLA/PEG/PHEBAMA nanoparticles were stored in DI water for characterization and measurements. The separated DMF solution of free polymer was purified by repeated centrifugation and precipitated with ethyl ether, and the resultant precipitate was dried in vacuum for molecular weight measurements.

3. RESULTS AND DISCUSSION

Figure 1 summarizes procedures for the preparation of SERS-active nanoparticles and the working mechanism for Cd^{2+} detection.

dx.doi.org/10.1021/cm201791r |*Chem. Mater.* 2011, 23, 4756–4764

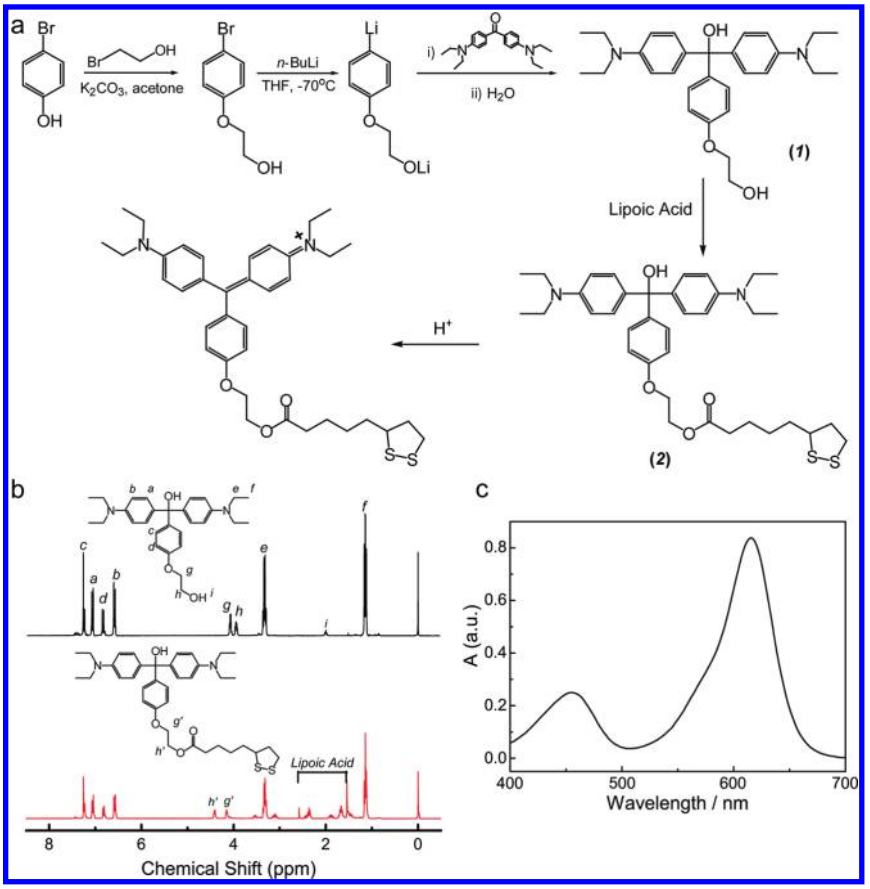

Figure 2. (a) Synthetic routes for the preparation of 2-(4-(bis(4-(diethylamino)phenyl)(hydroxy)methyl)phenoxy)ethanol (**1**) and 2-(4-(bis-(4-(diethylamino)phenyl)(hydroxy)methyl) phenoxy)ethyl 5-(1,2-dithiolan-3-yl)pentanoate (BGLA, **2**). (b) ^{1}H NMR spectra recorded for **1** and **2** in $CDCl_3$. (c) UV−vis spectrum recorded for the aqueous solution of BGLA (0.05 g/L, 25 °C) at pH 7.0.

Citrate-stabilized gold nanoparticles of 41 nm in diameter, which were synthesized in a two-step seeded growth procedure, were functionalized with a Raman active dye at first, followed by the coadsorption of methoxypoly(ethylene glycol)thiol (PEG-SH, MW = 2000 Da) and an ATRP initiator, 2,2′-dithiobis[1-(2-bromo-2-methyl-propionyloxy)]ethane (DTBE) through the Au−S bond. In previous studies, numerous Raman dyes such as IR-792 have been attached to nanoparticles surfaces through weak noncovalent interactions.[36−38,46] However, we found that DTBE used in the ligand exchange reaction can effectively remove weakly adsorbed IR-792 dyes since the formation of the Au−S bond is a much more favorable process compared to the noncovalent absorption of IR-792. To address this problem, we designed a new Raman dye containing brilliant green moiety and a disulfide anchoring group (Figure 1). The synthetic route of the new dye, named BGLA, is schematically illustrated in Figure 2, and the chemical structures of all the intermediates and the final product are confirmed by ^{1}H NMR and UV−vis spectroscopy. Briefly, 2-(4-bromophenoxy)ethanol was activated by *n*-butyllithium and then coupled with 4,4′-bis-(*N*,*N*-diethylamino)benzophenone, affording the brilliant green backbone, which were further reacted with lipoic acid to yield BGLA. In contrast to IR-792, BGLA can survive over the ligand exchange reaction by PEG and DTBE to remain on nanoparticle surfaces due to the strong multivalent interaction between the disulfide anchoring group and gold nanoparticle surfaces.[47,48] The short PEG chains are necessary to maintain the colloidal stability of gold nanoparticles during the ligand exchange reaction. Because both BGLA and DTBE are hydrophobic, the ligand exchange reaction at the surface of water-dispersible citrate-stabilized gold nanoparticles will result in the formation of insoluble aggregates in the absence of the PEG stabilizer. The free unbounded BGLA, DTBE, and PEG were removed by repeated centrifugation and washing, and the purified nanoparticles became dispersible in organic solvents including DMF, ethanol, and tetrahydrofuran, indicating a successful ligand exchange since the original nanoparticle cannot be dispersed in these solvents. As depicted in Figure 3, a new functional monomer, 2-(4-(2-hydroxyethylamino)-4-oxobutanamido)ethyl methacrylate (HEBAMA), containing two amide linkages, was synthesized via the amidation reaction of 2-aminoethyl methacrylate hydrochloride with 4-(2-hydroxyethylamino)-4-oxobutanoic acid (HEBA), which was prepared by the coupling of succinic anhydride and 2-aminoethanol. The design of HEBAMA is inspired by previous research on selective recognition of Cd^{2+} by polyamide groups. For example, Qian and co-workers reported a Cd^{2+} fluorescence sensor based on a BODIPY dye with four-armed polyamide chelating groups, which have shown selective affinity to Cd^{2+} with association constants K_{11} and K_{21} of 7.2×10^3 and 1.3×10^5, respectively.[8]

SI-ATRP has become a versatile tool to graft well-defined polymer brushes at the surface of functional nanoparticles.[39−42] In our recent study, amphiphilic gold nanoparticles have been produced by a tandem ligand exchange reaction and

dx.doi.org/10.1021/cm201791r |*Chem. Mater.* 2011, 23, 4756–4764

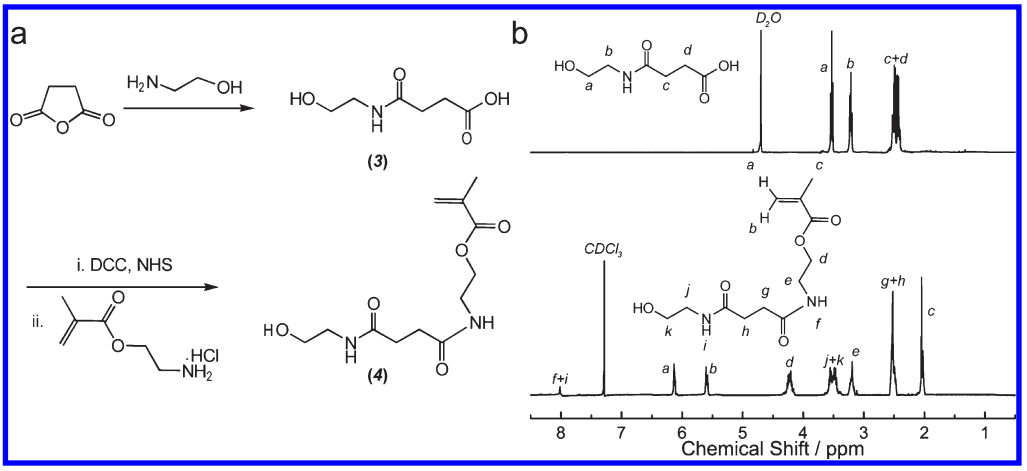

Figure 3. (a) Synthetic routes employed for the preparation of 4-(2-hydroxyethylamino)-4-oxobutanoic acid (HEBA, **3**) and 2-(4-(2-hydroxyethylamino)-4-oxobutanamido)ethyl methacrylate (HEBAMA, **4**). (b) ^{1}H NMR spectra recorded for **3** and **4** in D_2O and $CDCl_3$, respectively.

surface-initiated ATRP reaction, leading to smart nanoparticles coated with polymer brushes responsive to external stimuli such as pH.[41] Here, surface-initiated ATRP of HEBAMA was conducted in the presence of CuBr/Tris(2-(dimethylamino)ethyl)amine (Me_6TREN) in dimethylformide (DMF) at 50 °C, leading to hybrid nanoparticles coated with PEG and narrowly dispersed poly(HEBAMA) (PHEBAMA) chains (M_n = 21 kDa, M_w/M_n = 1.24). Our previous study showed that the sequential ligand exchange and surface-initiated ATRP reactions afforded hybrid nanoparticles with a polymer grafting density of 0.4−0.5 chain/nm^2, which corresponds to ∼2000 polymer chains at the surface of 41 nm gold nanoparticles.[41,42]

Polymer coatings have been widely used to endow nanoparticles with stimuli-responsiveness and improve the colloidal stability and biocompatibility of functional nanoparticles.[32,38−41,46−49] The SERS nanoparticles coated with hybrid brushes of PEG and PHEBAMA, which is highly water-soluble, exhibit a LSPR peak at 540 nm (Figure 4), red-shifted 8 nm relative to the citrate stabilized nanoparticles due to the higher refractive index of the polymer coating.[39] The LSPR peak remains unchanged in various buffer solutions such as phosphate buffered saline, confirming the excellent colloidal stability of the SERS nanoparticles. This is crucial for colloidal nanoparticle-based sensors because signal incurred by nonspecific aggregation can be effectively eliminated. In contrast, nanoparticles with small-molecular ligands typically exhibit low tolerance to the increased ionic strength of buffer solutions, and the aggregation because of poor colloidal stability often produce false signals.[22] Figure 4a shows that interparticle plasmonic coupling is immediately turned on upon the addition of Cd^{2+} ions (8 μM) in the SERS probe dispersion (12 pM). In the UV−vis spectra, a pronounced shoulder at 720 nm appears and its intensity gradually increases with increasing amount of Cd^{2+} added; at the same time, the intensity of the original LSPR peak at 540 nm progressively decreases, which is accompanied by a colorimetric red-to-blue transition. Transmission electron microscopy observation (Figure 4b) reveals that the SERS probe remained as dispersed single particles in the absence of Cd^{2+}, and addition of Cd^{2+} induced clustering of the probe to form large aggregates. Obviously, due to the significant difference in chain lengths of the two types of polymer grafts, the short PEG chain does not interfere with the binding of PHEBAMA with Cd^{2+}. SERS spectra of the corresponding solutions were captured under 785-nm laser excitation, showing dramatic increases in SERS signal intensities (Figure 4c) induced by the plasmonic coupling. For the Raman reporter BGLA, 633-nm laser excitation is preferred to achieve maximum signal amplification due to the resonance enhancement effect associated with its electronic transition at 616 nm (Figure 2c).[32] Meanwhile, previous work has shown that 633-nm and 785-nm laser excitations are favorable for well-dispersed single gold nanoparticles and nanoparticle aggregates, respectively.[37] Under the consideration of the above issues, 785-nm excitation is selected for a better off-on signal contrast. The SERS-active nanoparticles remain spectrally silent when staying as single particles and the SERS signal is only turned on upon forming aggregates. The SERS peak at 525 cm^{-1} corresponding to the ring skeletal vibration of radical orientation of the BGLA tag was used to determine the SERS enhancement factor. For example, 35 μM Cd^{2+} led to a 90-fold enhancement at 525 cm^{-1} in comparison with the background signal from single particles. We also found that using multiple Cd salts with different anions did not cause significant changes in the SERS spectroscopic profiles and the enhancement factors, indicating the potential uses of the SERS sensor for the detection of metal ions from different origins. When 12 pM aqueous dispersion of SERS-active gold nanoparticles is employed, the SERS probe in this study shows a detection limit of 1.0 μM (S/N = 3), which is comparable to that (0.6 μM) of the fluorescence sensor reported by Qian and co-workers.[8] Recently, Xue et al. described that a colorimetric sensor of Cd^{2+} based on gold nanoparticles stabilized with small molecular ligands, i.e., 6-mercaptonicotinic acid and L-cysteine displays a detection limit of 0.1 μM (S/N = 3) . However, it can be expected that the practical application of this kind of colorimetric sensors is limited by two practical issues: the poor colloidal stability of the nanoparticles and the inherent incapability of colorimetric assays for heavily colored samples. As shown in Figure 4e and f, our results have demonstrated that the SERS probe maintained its response to Cd^{2+} in the presence of the blue-colored complex of CuBr and N,N,N′,N′,N″-pentamethyldiethylenetriamine, although the UV−vis spectra and solution color showed little change. In addition, the combination of the SERS probe and portable Raman spectroscopy allows for onsite sampling and quantitative detection, offering unique advantages over other sensing schemes

dx.doi.org/10.1021/cm201791r |*Chem. Mater.* 2011, 23, 4756–4764

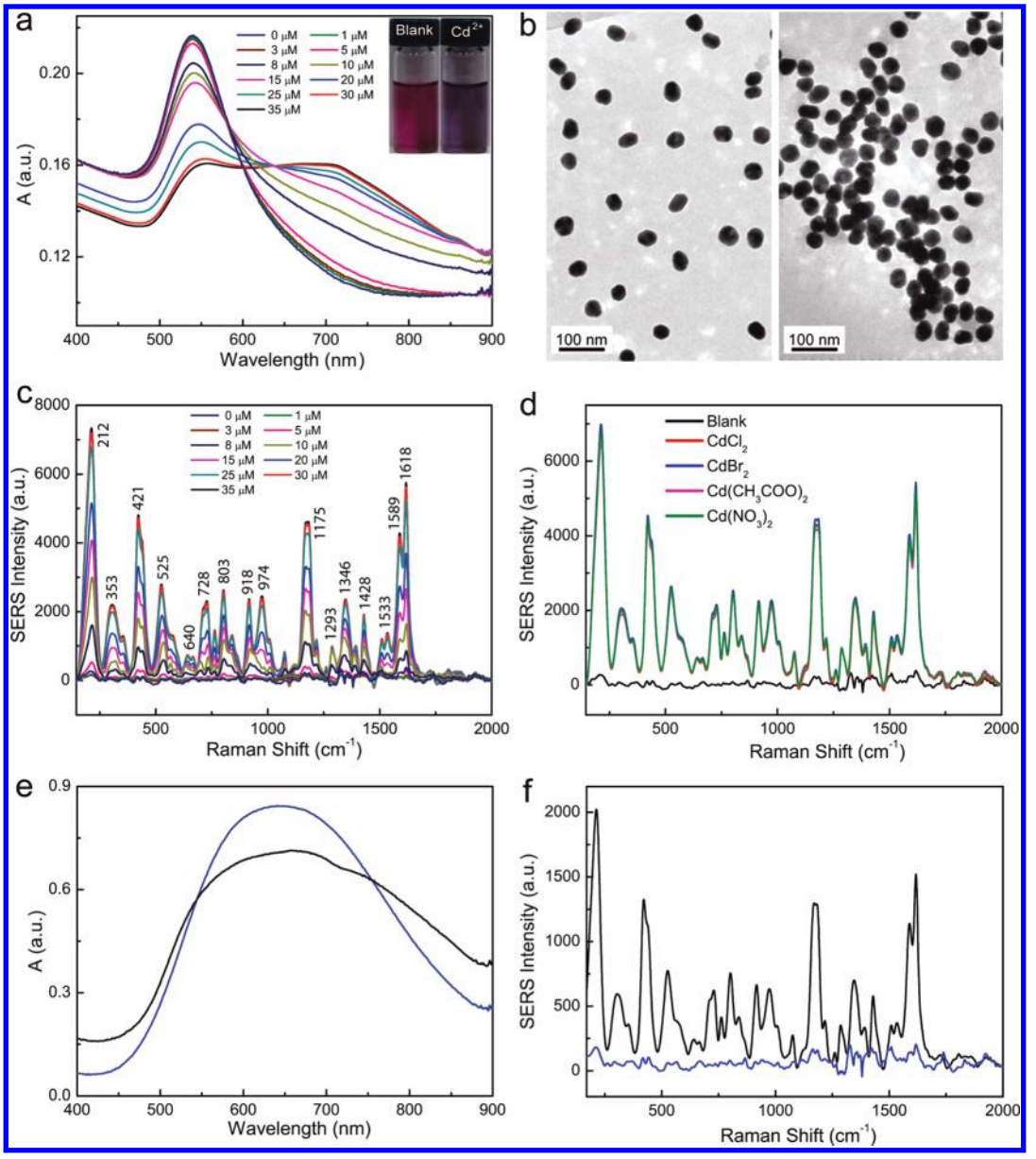

Figure 4. (a) UV−vis spectra recorded for aqueous dispersions (25 °C, pH 7; 12 pM) of Cd^{2+}-chelating polymer brush-coated SERS-active nanoparticles upon gradual addition of Cd^{2+} ions, and the inset shows photographs of the aqueous dispersion of SERS-active nanoparticles before and after Cd^{2+}addition (25 μM). (b) TEM images of the SERS nanoparticles at in absence (left) and 8 μM (right) of Cd^{2+} ions. (c) SERS spectra recorded for aqueous dispersions (25 °C, pH 7; 12 pM) of SERS-active nanoparticles upon gradual addition of Cd^{2+} ions. (d) SERS spectra of SERS-active nanoparticles in aqueous solutions of different Cd salts (25 μM). (e) SERS spectra recorded for aqueous dispersions (25 °C, pH 7; 12 pM) of Cd^{2+}-chelating polymer brush-coated SERS-active nanoparticles before and after addition of 8 μM Cd^{2+}. (f) UV−vis spectra measured for aqueous dispersions before and after addition of 8 μM Cd^{2+}. These two detections are performed in an aqueous medium obtained by mixing equal amount (500 μM) of CuBr and aqueous solution of PMDETA in deionized water and stirred for 30 min.

requiring bulky instruments such as atomic absorption spectrophotometry. For environmental applications, the current probe is highly useful for screening and monitoring burst release of Cd^{2+} ions.

The SERS nanoparticles also exhibit excellent selectivity for Cd^{2+} over various common metal ions. Figure 5 shows that, among the metal ions tested, Na^+, K^+, Cs^+, Ca^{2+}, Cu^{2+}, Pb^{2+}, Cr^{3+}, Fe^{2+}, and Hg^{2+} do not induce interparticle aggregation and the associated plasmonic coupling. Zn^{2+} has been the main source of interference for Cd^{2+} due to their similarity in terms of electronic structures.[7−9] At equivalent concentration (25 μM), Zn^{2+} results in a slight shoulder at ~720 nm in the LSPR spectrum (Figure 5a), and its intensity is considerably lower than that caused by Cd^{2+}. SERS measurement offers a more quantitative comparison (Figure 5b), revealing that the signal enhancement by Cd^{2+} is ~7 times of that by Zn^{2+}. While increased concentration (100 μM) of other metal ions still does not lead to detectable SERS signals (Figure 5c and d), the signal resulting from 100 μM Zn^{2+} increases to about 30% of that of 25 μM Cd^{2+}, suggesting a need for further optimizing the recognition ligand for better selectivity. A competitive assay (Figure 5e) using metal ions of 25 μM and 100 μM further demonstrates that Cd^{2+} can

dx.doi.org/10.1021/cm201791r |*Chem. Mater.* 2011, 23, 4756–4764

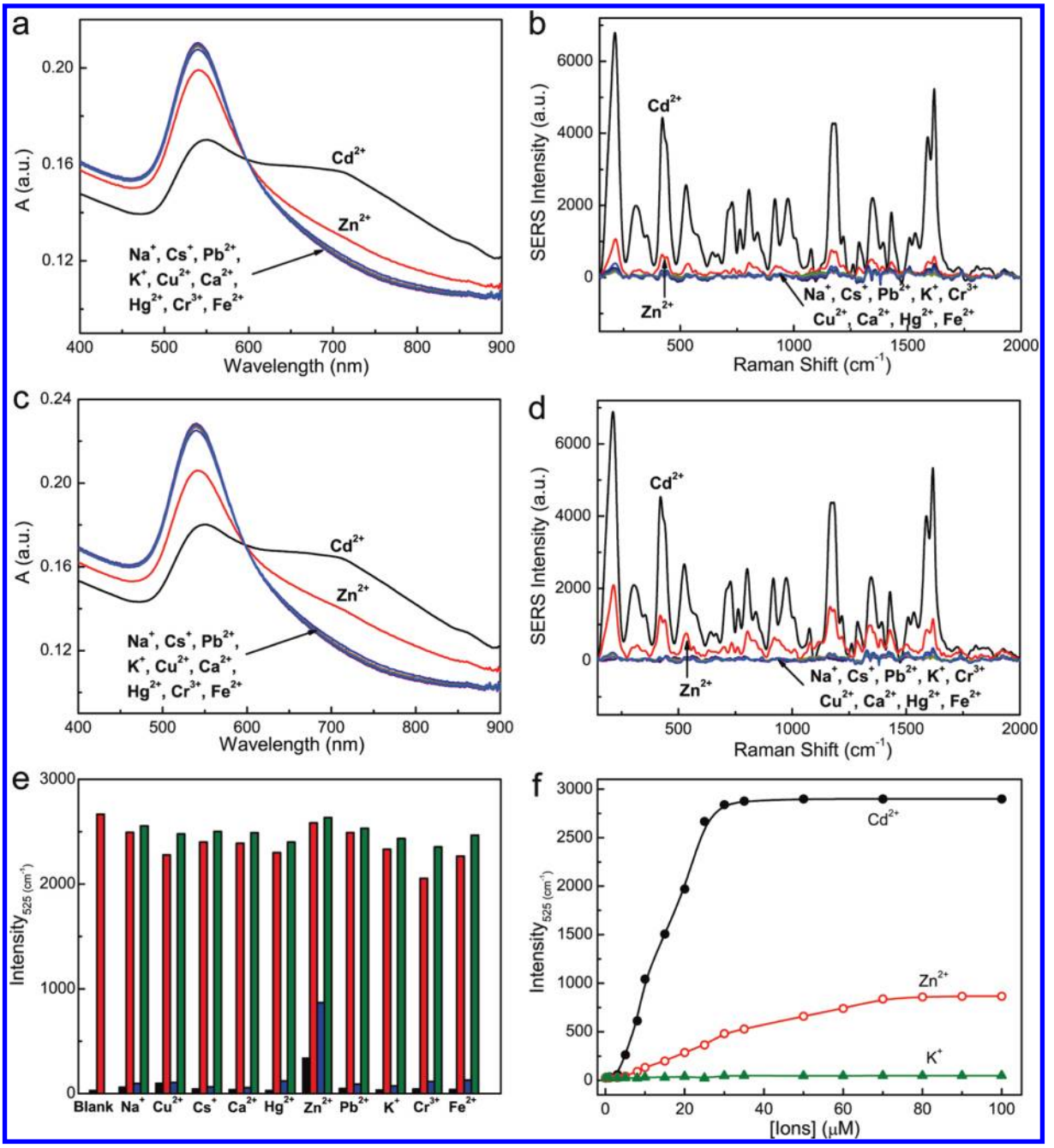

Figure 5. The detection selectivity of SERS-active nanoparticles. UV−vis spectra measured for aqueous dispersions (25 °C, pH 7; 12 pM) of the nanoparticle upon addition of 25 μM (a) and 100 μM (c) different metal ions (Na^+, Cs^+, Pb^{2+}, K^+, Cu^{2+}, Ca^{2+}, Hg^{2+}, Cr^{3+}, Fe^{2+}, Zn^{2+}, and Cd^{2+}). (b) SERS spectra recorded for the aqueous dispersions of SERS-active nanoparticles upon addition of 25 μM (b) and 100 μM (d) different metal ions. (e) The SERS intensity of the probes in 25 μM (black bars) and 100 μM (blue bars) competitive metal ions, and 25 μM Cd^{2+} ions in the presence of 25 μM (red bars) and 100 μM (green bars) competitive ions. (d) Metal ion (Cd^{2+}, Zn^{2+}, and K^+) concentration dependence of SERS signal intensity at 525 cm^{-1}.

effectively turn on the signal of the SERS nanoparticles premixed with other metal ions. In the presence of 25 μM competitive metal ions, equivalent Cd^{2+} (25 μM) leads to ~8 fold of signal enhancement for Zn^{2+} and ~50−90 fold for the rest of metal ions tested. The same concentration of Cd^{2+} give rise to ~3 fold of signal enhancement for 100 μM Zn^{2+}. Notably, the SERS signal (Figure 5f) of 12pM gold nanoparticle solution reaches the maximum at 25 μM Cd^{2+}, indicating the saturation of binding sites of the PHEBAMA brushes. Similarly, 70 μM Zn^{2+} also leads to the saturation, but the signal intensity is only comparable to that of 8 μM Cd^{2+}. Our SERS nanoparticles are densely grafted with mixed polymer brushes of long PHEBAMA chains and short PEG chains. This type of design can significantly increase the local concentration of Cd^{2+}-recognizing polyamide groups, which achieve a multivalent coordination effect and the observed superior detection selectivity. Previous work by Carron et al.[49] have used metal-chelating ligand modified Ag substrates for SERS detection of

dx.doi.org/10.1021/cm201791r |*Chem. Mater.* 2011, 23, 4756–4764

metal ions. Since the signal readout in that approach relies on the metal ion-binding induced spectral shifts (10−20 cm^{-1}) of the ligand, it is very challenging to translate the signal changes for specific metal ions and avoid interference from competitive species when used in complex medium. In comparison, the Raman tag and polymer brushes in our design serve for signaling and metal ion recognition separately, and the quantification is exclusively based on the fingerprint signal of the Raman tag and its enhancement generated by aggregation of the nanoparticle scaffolds, thus allowing for easy signal readout and assignment.

4. CONCLUSIONS

In summary, we have presented a new design of highly sensitive and selective SERS nanosensors for Cd^{2+}, based on the use of a new Raman reporter dye with a disulfide anchoring group, a new polymer ligand for specific Cd^{2+} chelating, and surface-initiated ATRP for the surface coating preparation. The narrow SERS signature peaks, integrated with the ability of ATRP for controlled polymerization of versatile monomers, offers new possibilities to develop an array of SERS nanoparticles for multiplex detection of multiple metal ions of interest simultaneously. The development of portable Raman spectroscopy eliminates the need for bulky instruments in other sensing schemes, providing the opportunity to perform onsite sampling and quantitative detection.

AUTHOR INFORMATION

Corresponding Author

*E-mail: hduan@ntu.edu.sg (H.D.); sliu@ustc.edu.cn (S.L.).

ACKNOWLEDGMENT

H.D. acknowledges the program of Nanyang Assistant Professorship for financial support. This work is supported in part by a NIG grant (NMRC/NIG/0022/2008) to R. X. from the National Medical Research Council (Singapore).

REFERENCES

(1) Turner, A. P. F. *Science* **2000**, *290*, 1315–1317.
(2) Domaille, D. W.; Que, E. L.; Chang, C. J. *Nat. Chem. Biol.* **2008**, *4*, 168–175.
(3) Tsien, R. W.; Tsien, R. Y. *Annu. Rev. Cell Biol.* **1990**, *6*, 715–760.
(4) Liu, J.; Qu, W.; Kadiiska, M. B. *Toxicol. Appl. Pharmacol.* **2009**, *238*, 209–214.
(5) Dong, Z. W.; Wang, L.; Xu, J. P.; Li, Y. L.; Zhang, Y.; Zhang, S.; Miao, J. Y. *Toxicol. in Vitro* **2009**, *23*, 105–110.
(6) He, Q. W.; Miller, E. W.; Wong, A. P.; Chang, C. J. *J. Am. Chem. Soc.* **2006**, *128*, 9316–9317.
(7) Peng, X. J.; Du, J. J.; Fan, J. L.; Wang, J. Y.; Wu, Y. K.; Zhao, J. Z.; Sun, S. G.; Xu, T. *J. Am. Chem. Soc.* **2007**, *129*, 1500–1501.
(8) Cheng, T. Y.; Xu, Y. F.; Zhang, S. Y.; Zhu, W. P.; Qian, X. H.; Duan, L. P. *J. Am. Chem. Soc.* **2008**, *130*, 16160–16161.
(9) Xue, L.; Liu, C.; Jiang, H. *Org. Lett.* **2009**, *11*, 1655–1658.
(10) Ding, L.; Cheng, W.; Wang, X. J.; Ding, S. J.; Ju, H. X. *J. Am. Chem. Soc.* **2008**, *130*, 7224–7225.
(11) Yin, J.; Guan, X. F.; Wang, D.; Liu, S. Y. *Langmuir* **2009**, *25*, 11367–11374.
(12) Qian, X. H.; Xiao, Y.; Xu, Y. F.; Guo, X. F.; Qian, J. H.; Zhu, W. P. *Chem. Commun.* **2010**, *46*, 6418–6436.
(13) Choi, Y.; Park, Y.; Kang, T.; Lee, L. P. *Nat. Nanotechnol.* **2009**, *4*, 742–746.
(14) Lee, J. S.; Han, M. S.; Mirkin, C. A. *Angew. Chem., Int. Ed.* **2007**, *46*, 4093–4096.
(15) Liu, J. W.; Lu, Y. *J. Am. Chem. Soc.* **2004**, *126*, 12298–12305.
(16) Li, H. B.; Yao, Y.; Han, C. P.; Zhan, J. Y. *Chem. Commun.* **2009**, 4812–4814.
(17) Liu, D. B.; Qu, W. S.; Chen, W. W.; Zhang, W.; Wang, Z.; Jiang, X. Y. *Anal. Chem.* **2010**, *82*, 9606–9610.
(18) Lin, S. Y.; Wu, S. H.; Chen, C. H. *Angew. Chem., Int. Ed.* **2006**, *45*, 4948–4951.
(19) Huang, C. C.; Yang, Z.; Lee, K. H.; Chang, H. T. *Angew. Chem., Int. Ed.* **2007**, *46*, 6824–6828.
(20) Kalluri, J. R.; Arbneshi, T.; Khan, S. A.; Neely, A.; Candice, P.; Varisli, B.; Washington, M.; McAfee, S.; Robinson, B.; Banerjee, S.; Singh, A. K.; Senapati, D.; Ray, P. C. *Angew. Chem., Int. Ed.* **2009**, *48*, 9668–9671.
(21) Kim, S.; Park, J. W.; Kim, D.; Kim, D.; Lee, I. H.; Jon, S. *Angew. Chem., Int. Ed.* **2009**, *48*, 4138–4141.
(22) Xue, Y.; Zhao, H.; Wu, Z. J.; Li, X. J.; Ye, Y. J.; Yuan, Z. B. *Analyst* **2011**, *136*, 3725–3730.
(23) Jain, P. K.; Huang, X. Y.; El-Sayed, I. H.; El-Sayed, M. A. *Acc. Chem. Res.* **2008**, *41*, 1578–1586.
(24) Halas, N. J. *Nano Lett.* **2010**, *10*, 3816–3822.
(25) Choi, C. L; Alivisatos, A. P. *Annu. Rev. Phys. Chem.* **2010**, *61*, 369–389.
(26) Camden, J. P.; Dieringer, J. A.; Zhao, J.; Van Duyne, R. P. *Acc. Chem. Res.* **2008**, *41*, 1653–1661.
(27) Qian, X. M.; Nie, S. M. *Chem. Soc. Rev.* **2008**, *37*, 912–920.
(28) Banholzer, M. J.; Millstone, J. E.; Qin, L. D.; Mirkin, C. A. *Chem. Soc. Rev.* **2008**, *37*, 885–897.
(29) Alvarez-Puebla, R. A.; Liz-Marzan, L. M. *Small* **2010**, *6*, 604–610.
(30) Shafer-Peltier, K. E.; Haynes, C. L.; Glucksberg, M. R.; Van Duyne, R. P. *J. Am. Chem. Soc.* **2003**, *125*, 588–593.
(31) Cao, Y. W. C.; Jin, R. C.; Mirkin, C. A. *Science* **2002**, *297*, 1536–1540.
(32) Qian, X. M.; Peng, X. H.; Ansari, D. O.; Yin-Goen, Q.; Chen, G. Z.; Shin, D. M.; Yang, L.; Young, A. N.; Wang, M. D.; Nie, S. M. *Nat. Biotechnol.* **2008**, *26*, 83–90.
(33) Gehan, H.; Fillaud, L.; Chehimi, M. M.; Aubard, J.; Hohenau, A.; Felidj, N.; Mangeney, C. *ACS Nano* **2010**, *4*, 6491–6500.
(34) Wustholz, K. L.; Henry, A. I.; McMahon, J. M.; Freeman, R. G.; Valley, N.; Piotti, M. E.; Natan, M. J.; Schatz, G. C.; Van Duyne, R. P. *J. Am. Chem. Soc.* **2010**, *132*, 10903–10910.
(35) Yang, M.; Alvarez-Puebla, R.; Kim, H. S.; Aldeanueva-Potel, P.; Liz-Marzan, L. M.; Kotov, N. A. *Nano Lett.* **2010**, *10*, 4013–4019.
(36) Graham, D.; Thompson, D. G.; Smith, W. E.; Faulds, K. *Nat. Nanotechnol.* **2008**, *3*, 548–551.
(37) Qian, X. M.; Zhou, X.; Nie, S. M. *J. Am. Chem. Soc.* **2008**, *130*, 14934–14935.
(38) Qian, X. M.; Li, J.; Nie, S. M. *J. Am. Chem. Soc.* **2009**, *131*, 7540–7541.
(39) Duan, H. W.; Kuang, M.; Wang, D. Y.; Kurth, D. G.; Mohwald, H. *Angew. Chem., Int. Ed.* **2005**, *44*, 1717–1720.
(40) Li, D. X.; He, Q.; Cui, Y.; Li, J. B. *Chem. Mater.* **2007**, *19*, 412–417.
(41) Cheng, L.; Liu, A. P.; Peng, S.; Duan, H. W. *ACS Nano* **2010**, *4*, 6098–6104.
(42) Cheng, L.; Song, J. B.; Yin, J.; Duan, H. W. *J. Phys. Chem. Lett.* **2011**, *2*, 2258–2262.
(43) Ciampolini, M.; Nardi, N. *Inorg. Chem.* **1966**, *5*, 41–44.
(44) Jiang, Y. G.; Wang, Y. P.; Ma, N.; Wang, Z. Q.; Smet, M.; Zhang, X. *Langmuir* **2007**, *23*, 4029–4034.
(45) Yin, J.; Ge, Z. S.; Liu, H.; Liu, S. Y. *J. Polym. Sci., Part A: Polym. Chem.* **2009**, *47*, 2608–2619.
(46) von Maltzahn, G.; Centrone, A.; Park, J. H.; Ramanathan, R.; Sailor, M. J.; Hatton, T. A.; Bhatia, S. N. *Adv. Mater.* **2009**, *21*, 3175–3180.

(47) Stewart, M. H.; Susumu, K.; Mei, B. C.; Medintz, I. L.; Delehanty, J. B.; Blanco-Canosa, J. B.; Dawson, P. E.; Mattoussi, H. *J. Am. Chem. Soc.* **2010**, *132*, 9804–9813.
(48) Song, J. B.; Cheng, L.; Liu, A. P.; Yin, J.; Kuang, M.; Duan, H. W. *J. Am. Chem. Soc.* **2011**, *133*, 10760–10763.
(49) Duan, H. W.; Kuang, M.; Wang, Y. A. *Chem. Mater.* **2010**, *22*, 4372–7378.
(50) Crane, L. G.; Wang, D. X.; Sears, L. M.; Heyns, B.; Carron, K. *Anal. Chem.* **1995**, *67*, 360–364.